DETECTION OF NEW DEEP MOONQUAKES IN THE APOLLO LUNAR SEISMIC DATA: IMPLICATIONS FOR TEMPORAL AND SPATIAL DISTRIBUTION. R. C. Bulow[1], C. L. Johnson[1], and P. M. Shearer[1] [1]Cecil H. and Ida M. Green Institute of Geophysics and Planetary Physics, Scripps Institution of Oceanography, University of California, San Diego. 9500 Gilman Drive, La Jolla, CA 92093-0225, renee@ucsd.edu

Introduction and Overview: The Apollo Passive Seismic Experiment consisted of four seismometers deployed on the lunar surface between 1969 and 1972. Data were recorded continuously until 1977, and approximately 12,000 seismic events were detected [1]. These events were classified into three main types: impacts, shallow moonquakes, and deep moonquakes. The latter comprise nearly half of the catalogued events. Early studies of these deep events revealed 77 separate source regions, each of which produces a characteristic waveform [2]. Deep moonquakes were also discovered to occur with tidal periodicity [3].

The repeatability of waveforms from a single source region can be used to search for new events in the continuous data via cross-correlation. Because the original events were selected from the continuous data by eye, automating the process allows us not only to detect signals close to the noise level, but also to classify some of the catalogued events not previously associated with any group. This search fills out the event catalog, providing a complete description of deep moonquake occurrence times for identified clusters, from which improved estimates of tidal periodicities can be made.

Waveform repeatability can also be used for stacking events from a single source region. This improves signal-to-noise (SNR) and the visibility of seismic phases. Our event search improves stack quality by increasing the total number of events in a given stack. Optimized stacks are produced using a weighted iterative approach. This reduces erroneous trace selection and creates the cleanest possible stacks from which travel times estimates can be made. We use these travel times to estimate source region locations and compare to those of previous studies.

New Event Search: Our method is illustrated through analyses of the A1 deep event group, the largest of the previously-identified source regions. However, the approach is general and can be extended to other deep clusters. To begin the search, we first create a target stack from selected catalogued A1 events. Events to be stacked are chosen by cross-correlating all catalogued A1 events with each other. “Good” correlations are identified using a minimum correlation coefficient cutoff and by checking for small time shifts relative to the original catalog time. An absolute correlation coefficient of 0.2 yields an average standard deviation in time shifts less than 0.1 seconds, which is smaller than the data sampling interval. Events meeting these criteria are stacked. The percentage of catalogued events in the stack for a given station and channel ranges from 17% to 71%. This stack becomes the “target trace” for cross-correlation, or the trace with which the continuous data will be compared.

Once the target trace has been created, a 20-minute window from the target (starting with the onset of the event) is cross-correlated with the continuous time series. Instances where the correlation coefficient falls above a specified cutoff are noted and compared to the catalog of known events. Times not appearing in the catalog indicate a possible new event in the continuous data. Because small events may not appear on every station, correlations are performed separately for every channel and station.

To determine which correlations represent real events, we perform cross-correlations in which the target trace is time-reversed. This gives a target trace with the same amplitude and frequency content as the real trace but with physically meaningless phase behavior. Cross-correlation peaks resulting from time-reversed targets are judged to be “false" peaks that provide a measure of the absolute correlation coefficient associated with noise. The correlation cutoff for each channel is set to the absolute maximum coefficient returned by these time-reversed correlations. Points falling above this cutoff in the real calculation represent new events. New events identified on each station and channel are summarized in Table 1.

Table 1: New events per station/channel

station	lpx	lpy	lpz
12	67	67	54
14	48	70	4
15	9	17	6
16	40	41	16

Because many of the events in Table 1 are not unique, we need to define what constitutes a new event. We do this as follows: for every event shown in Table 1, we require that it appear on at least *n* of the 12 long-period channels. We also investigate the use of different correlation cutoffs, defined as

multiple values of the absolute maximum value returned by the time-reversed correlations. Experimentation with different *n* values and cutoff multipliers (Figure 1) gave good results for *n*=2 and a multiplier of 1, resulting in 101 total new A1 events. This represents a 56% increase in the total number of catalogued A1 events.

Figure 1: Determining number of new events

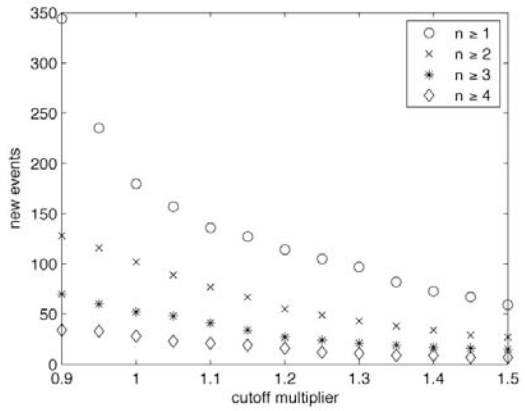

Stack Optimization: Because A1 events in the original catalog are of variable quality, stacking these events using a simple arithmetic average of traces may not produce as clean a stack as a method which gives more weight to highly-correlating traces or those having a better SNR. We employ a weighted iterative stacking method to ensure events are selected and stacked to create a representative trace with high SNR and the clearest seismic phase arrivals. Using a single high-quality A1 event as the target trace, we perform cross-correlations with all catalogued events, including those discovered in the new event search.

Events correlating with the target at 0.2 or higher are considered for stacking. Before the stack is formed, each individual trace is weighted by the squared correlation coefficient, r^2. We also attempted weighting by r, higher powers of r, and the SNR, but weighting with r^2 produced a stack with the most easily discernable seismic phase arrivals.

The cross-correlation procedure is then repeated using the weighted stack as the target. To optimize the stack, the process is repeated until the number of events added to the stack stabilizes. We find good convergence after four iterations.

Travel-time picks: P- and S-wave arrival picks made from our optimized A1 stacks are shown for station 12 in Figure 2. Our S-P differential times show good agreement with comparison times from two reference publications [4,5] as summarized in Table 2. This is to be expected, as A1 is the largest and most-studied deep cluster. Application of our method to less well-characterized clusters [4,5] will be of particular interest.

Figure 2: A1 optimized stacks with picks

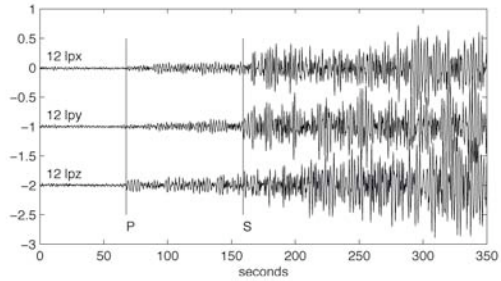

Table 2: S-P differential times in seconds

station	this study	ref. [4]	ref. [5]
12	91.5	99.7	98.1
14	106.0	103.2	105.8
15	141.4	148.1	145.8
16	138.9	137.9	138.1

Spatial and Temporal Distribution of Deep Moonquakes: We use our travel time picks to estimate deep cluster locations. Initially we use previously published seismic velocity estimates [4,5] and an adaptive grid search algorithm to identify the best-fit location. As expected, based on the similar differential travel times our location estimates for A1 are quite similar to those obtained previously. However, the more accurate travel-time picks mean that uncertainties in our estimates of deep cluster locations and variations among different estimates reflect mainly the spatial extent of the source region and trade-offs with seismic velocity structure. Clusters with previously disparate location estimates may be better located after our new event search.

The 56% increase in A1 events resulting from our new event search allows improved estimates of the dominant periodicities in the data. We will explore tidal signals present in this and other clusters, characterizing their phase behavior in the time domain. For the largest clusters, spectral analyses may be attempted. The results from this analysis will provide the data for future tidal stress modeling of the deep moonquakes.

References: [1] Nakamura, Y. et al. (1981) *Galveston Geophysics Laboratory Contribution No. 491*, Tech. Rept. No. 18. [2] Nakamura, Y. (2003) *Phys. Earth Planet. Int., 139*, 197-205. [3] Lammlein, D. R. (1977) *Phys. Earth Planet. Int., 14*, 224-273. [4] Nakamura, Y. (1983) *JGR, 88*, 677-686. [5] Lognonné, P. et al. (2003) *Earth Planet. Sci. Letters, 211*, 27-44.